STEM CELLS®

EMBRYONIC STEM CELLS/INDUCED PLURIPOTENT STEM CELLS

Chromosome Transplantation: Correction of the Chronic Granulomatous Disease Defect in Mouse Induced Pluripotent Stem Cells

ALESSANDRA CASTELLI,[a,b] LUCIA SUSANI,[a,b] CIRO MENALE,[a,b] SHARON MUGGEO,[a,b] ELENA CALDANA,[a,b] DARIO STRINA,[a,b] BARBARA CASSANI,[a,b] CAMILLA RECORDATI,[c] EUGENIO SCANZIANI,[c] FRANCESCA FICARA,[a,b] ANNA VILLA,[a,d] PAOLO VEZZONI,[a,b,*] MARIANNA PAULIS[a,b,*]

Key Words. Chronic granulomatous disease • Induced pluripotent stem cells • CRISPR/Cas system • X-linked combined immunodeficiency diseases • Genetic therapy

[a]National Research Council (CNR)—IRGB/UOS of Milan, Milan, Italy; [b]Humanitas Clinical and Research Center—IRCCS, Rozzano, Milan, Italy; [c]Department of Veterinary Sciences and Public Health, University of Milan, Milan, Italy; [d]San Raffaele Telethon Institute for Gene Therapy (SR-TIGET), IRCCS San Raffaele Scientific Institute, Milan, Italy

[*]Jointly supervised this work.

Correspondence: Marianna Paulis, Ph.D., Humanitas Clinical and Research Center—IRCCS, Rozzano, Milan, Italy. Telephone: 39-02-82245164; e-mail: marianna.paulis@humanitasresearch.it

Received August 1, 2018; accepted for publication March 12, 2019; first published online March 20, 2019.

http://dx.doi.org/10.1002/stem.3006

ABSTRACT

In spite of the progress in gene editing achieved in recent years, a subset of genetic diseases involving structural chromosome abnormalities, including aneuploidies, large deletions and complex rearrangements, cannot be treated with conventional gene therapy approaches. We have previously devised a strategy, dubbed chromosome transplantation (CT), to replace an endogenous mutated chromosome with an exogenous normal one. To establish a proof of principle for our approach, we chose as disease model the chronic granulomatous disease (CGD), an X-linked severe immunodeficiency due to abnormalities in *CYBB* (*GP91*) gene, including large genomic deletions. We corrected the gene defect by CT in induced pluripotent stem cells (iPSCs) from a CGD male mouse model. The *Hprt* gene of the endogenous X chromosome was inactivated by CRISPR/Cas9 technology thus allowing the exploitation of the hypoxanthine–aminopterin–thymidine selection system to introduce a normal donor X chromosome by microcell-mediated chromosome transfer. X-transplanted clones were obtained, and diploid XY clones which spontaneously lost the endogenous X chromosome were isolated. These cells were differentiated toward the myeloid lineage, and functional granulocytes producing GP91 protein were obtained. We propose the CT approach to correct iPSCs from patients affected by other X-linked diseases with large deletions, whose treatment is still unsatisfactory. STEM CELLS *2019;37:876–887*

SIGNIFICANCE STATEMENT

A lot of genetic diseases involving chromosome abnormalities cannot be treated by conventional gene therapy approaches. This study applied chromosome transplantation, a new genomic therapy method that has been recently developed, to induced pluripotent stem cells (iPSCs) derived from an X-linked mouse disease model. As a proof of principle, this study demonstrated that X-chromosome-transplanted corrected cells restored the normal function to differentiated cells. Although all the strategies based on iPSCs are still far away from the clinic, it is believed that the results establish an important step for the usefulness of this kind of genomic therapy in selected patients.

INTRODUCTION

Chromosome transplantation (CT) is a new approach to correct genomic defects based on the precise exchange of an endogenous defective chromosome with a normal exogenous one [1]. Theoretically, this approach could restore any genetic disease, but the technical difficulties of transferring intact chromosomes and concomitantly eliminating the defective endogenous one, have dissuaded researchers to extensively pursue this approach, since gene therapy methods based on viral vectors and more recently on programmable nucleases are more feasible. However, a subset of structural abnormalities are impossible to correct using these strategies. They include aneuploidies, large deletions, inversions, and defects due to large triplet expansions that cause "genomic disorders" [2]. Recently, the attempt to treat these diseases have established the new field of "chromosome or genomic therapy" [1, 3–6].

We have recently shown, as proof of principle, that it is possible to substitute in mouse

embryonic stem cells (ESCs) the *Hprt*-defective X chromosome with a *wild-type* (*wt*) one [1], thus correcting the genetic defect that in humans causes the Lesch–Nyhan syndrome. The *Hprt* gene was chosen since $Hprt^{+}$ and $Hprt^{-}$ cells can be easily selected in vitro allowing the identification of corrected cells: $Hprt^{+}$ cells survive in hypoxanthine–aminopterin–thymidine (HAT) medium, whereas $Hprt^{-}$ cells survive in 6-thioguanine (6-TG) medium. Therefore, in principle, any X-linked disease in which *Hprt* has been inactivated by gene targeting, could be easily selected taking advantage of the HAT selection system. X chromosome is involved in several important human diseases, which at present cannot be efficiently treated with standard gene therapy methods. Examples include Duchenne dystrophy (DD), often caused by large deletions, whose treatment is still unsatisfactory in spite of recent progress [7, 8], Fragile X syndrome, in which reduction of the triplet expansion with normalization of gene expression has only partially been achieved [9], and Turner syndrome, in which a normal diploid content could be restored by an X chromosome transfer [10].

In the present paper, we show as a proof of principle that this approach is able to correct the genetic defect in induced pluripotent stem cells derived from a mouse model of chronic granulomatous disease (CGD-iPSCs) [11], a severe disease of the immune system due to mutations in the *CYBB* gene [12]. The protocol used can correct any genetic defect involving the X chromosome [10], maintaining intact all the regulatory elements and leaving no mark of the procedure. The CGD mouse model was chosen since large deletions in the *CYBB* gene are found in 10% to 15% of patients [13]. CYBB is a component of the nicotinamide adenine dinucleotide phosphate (NADPH) enzymatic complex that is critical for phagocyte killing of bacteria through reactive oxygen species. Due to this deficiency, phagocytes from CGD patients are present but not-functional [14, 15].

Materials and Methods

Animal Use and Care

B6.129S-Cybb^{tm1Din}/J mutant mice [11] and C57BL/6 *wt* mice were maintained according to the Italian regulations (D.L. n.116, G.U., suppl. 40, 18 febbraio 1992, Circolare no. 8, G.U. 14-luglio 1994D.Lgs. 26/2014) and EU Directive guidelines (2010/63/EU). NOD.Cg-Prkdc^{scid} Il2rg^{tm1Wjl}/SzJ (NSG) mice were purchased from Charles River Laboratories (Calco, Italy). GFP^{+} C57BL/6 were produced in our laboratory by crossing C57 mice to the GFP^{+} [16]. The study was approved by the Italian Ministry of Health (approval no. 45/2015-PR). The experimental facility was maintained at 23°C (±0.5°C). The light cycle was set at 14/10 hours (light/dark). Animals were given ad libitum access to food and water.

Cell Cultures

Mouse embryonic fibroblasts (MEFs) were obtained by mincing and dissociating 13.5 days post coitum (dpc) CD-1 embryos (Charles River Laboratories) by Trypsin-Versene (Lonza, Basel, Switzerland). Primary cultures were maintained in high glucose Dulbecco's modified Eagle's medium (DMEM) supplemented with 10% fetal calf serum (FCS, Lonza).

The A9/MEF-C12 hybrid cell line was obtained by cell fusion between A9 cells and MEF cells [1] and maintained by standard culture procedures in DMEM medium, supplemented with 10% FCS and HAT medium (Sigma–Aldrich, St. Louis, MO).

Mouse iPSCs and their derivative hybrid cells were cultured on mitomycin-C (Sigma–Aldrich) treated MEF feeder layer in standard mouse iPSC medium: knockout DMEM (KO-DMEM; Thermo Fisher Scientific, Waltham, MA) containing 15% ESC-qualified FCS (Thermo Fisher Scientific), 1,000 U/ml leukemia-inhibitory factor (LIF-ESGRO Chemicon, Merck Millipore, Darmstadt, Germany), 0.1 mM nonessential amino acids (Lonza), 2 mM L-glutamine (Lonza), 50 μg/ml penicillin–streptomycin (Lonza), and 100 μM β-mercaptoethanol (Thermo Fisher Scientific).

iPSC Generation and Expansion

Wild-type and CGD cells were reprogrammed using the integration-free CytoTune-iPS 2.0 Sendai Reprogramming Kit (Thermo Fisher Scientific), which contains Sendai virus particles of the four Yamanaka factors [17]. Briefly, $cKit^{+}$ hematopoietic progenitor cells from the mouse CGD bone marrow (BM) were plated onto wells of a gelatin-coated 6-well plate 24 hours before viral transduction. The cells were transduced according to the manufacturer protocol. Four days after transduction, cells were plated onto MEF feeder cells, and fed with mouse iPSC medium. Approximately 7 days after plating, the first appearing colonies were picked for expansion into individual iPSC lines, transferred to MEF feeder cells and cultured with iPSC medium. At least three iPSC colonies from each cell line were expanded and analyzed for pluripotency and karyotype stability.

CRISPR/Cas9 Transfection and 6-TG Selection

Cells were seeded into 6-well plates (approximately 2×10^5 cells per well) and transfections were performed using Lipofectamine 2000 (Thermo Fisher Scientific) according to the manufacturer's protocol. To target the mutation in the *Hprt* gene, CGD-iPSCs were cotransfected with two vectors previously described [18, 19]. Briefly, 1 μg of CRISPR/Cas9 pX330 plasmid containing a guide-RNA (gRNA) specific for the exon 3 of the *Hprt* gene (gRNA-Ex3-*Hprt*) was cotransfected with 1 μg of pPNT-HPRT construct containing the TK gene from the Herpes Simplex Virus Thymidine Kinase (HSV-TK) and a neomycin selectable marker, flanked by two homologous arms from the *Hprt* gene. After 48 hours, transfected cells were seeded at low density (6×10^4 cells per p100), selected in 6-TG medium (30 μM, Sigma–Aldrich) and pooled together.

Microcell Mediated Chromosome Transfer and Clone Isolation

Microcell mediated chromosome transfer (MMCT) from the A9/MEF-C12 hybrid donor cell line to unsynchronized recipient mouse 6-TG^{R} CGD-iPSCs was performed as previously described with minor modifications [1]. In brief, approximately 5×10^6 mouse A9/MEF-C12 hybrid cells were plated on six gelatin-coated high-speed polycarbonate centrifuge tubes (Nalgene, Rochester, NY) and used as source of microcells for the MMCT. To promote micronuclei formation, cells were treated with 0.2 μg/ml of colcemid (KaryoMAX, Thermo Fisher Scientific). After 48 hours of incubation, the medium was replaced with DMEM medium containing cytochalasin B (10 μg/ml, Sigma–Aldrich) and the tubes were centrifuged at 16,000*g* for 70 minutes at 37°C. The pellet containing extruded microcells were resuspended in 10 ml of serum-free DMEM and purified

by two consecutive filtrations using membranes with 8 μm pores (Millipore). 1–3 × 10^7 purified microcells were collected by centrifugation at 400*g* for 10 minutes, resuspended in 2 ml of serum-free DMEM and then mixed with 10^7 monodispersed mouse 6-TG^R CGD-iPSCs. After centrifugation at 160*g*, 1 ml of a prewarmed solution of 50% PEG 1500 (Roche, Mannheim, Germany) was poured onto the cell pellet over 1 minute, followed by extensive washing in serum free DMEM. 2.5 × 10^6 cells were plated in p100 dishes and after 48 hours 1× HAT selection was added.

Chromosome Preparation and Analysis

Chromosome analysis was carried out on slide preparations of cell suspensions. Briefly, cell cultures were treated with KaryoMAX at a final concentration of 0.1 μg/ml for 2 hours at 37°C and mitoses were collected. After hypotonic treatment and fixation in methanol: acetic acid solution (3:1 vol/vol), each cell suspension was dropped onto a slide and air-dried. Chromosome counts and karyotype analyses were done on metaphases stained with Vectashield mounting medium with DAPI (Vector Laboratories, Youngstown, OH) for DAPI banding.

Images were captured using an Olympus BX61 Research Microscope (Olympus Diagnostics, London) equipped with a cooled CCD camera and analyzed with Applied Imaging Software CytoVision for mouse karyotyping (CytoVision; Applied Imaging, Santa Clara, CA).

FISH

Flow-sorted DNA for X chromosome (M.A. Ferguson-Smith, University of Cambridge, Cambridge, U.K.) was labeled via PCR with Spectrum Orange-dUTP (Vysis, IL). The pPNT vector containing the TK gene, and BAC RP23-173F3 containing the *Hprt* gene, were labeled via nick translation (Thermo Fisher Scientific) using biotin-16-dUTP (Roche) and used as DNA probes.

The labeled probes were resuspended in hybridization buffer (50% formamide, 10% dextran sulphate, 1× Denhardt's solution, 0.1% SDS, 40 mM Na_2HPO_4 pH 6.8, 2× SSC) containing 10× mouse Cot1 DNA (Thermo Fisher Scientific) and denatured at 80°C for 10 minutes. In situ hybridization was performed as previously described [20]. In brief, slides were treated with Pepsin (0.004%) at 37°C for 30 seconds and dehydrated through the ethanol series before denaturation in 70% formamide/2× SSC. Hybridization was completed overnight at 37°C. Stringent washes were carried out in 0.4% SSC at 72°C for 5 minutes. Slides were mounted in Vectashield mounting medium with DAPI and then were scored under an Olympus BX61 Research Microscope equipped with a cooled CCD camera. Images were captured and analyzed with Applied Imaging Software CytoVision (CytoVision Master System with Karyotyping & FISH). To identify the pPNT vector localization at least 50 cells were analyzed.

Alkaline Phosphatase Staining

Leucocyte Alkaline Phosphatase Kit (Sigma–Aldrich) was used, accordingly to kit instructions.

Embryoid Body Formation

A total of 1,000 mouse iPSCs were cultured in hanging drops (20 μl) on covers of 100 mm hydrophobic dishes in differentiation medium (iPSC medium without LIF). After 2/3 days of incubation, the drops were transferred to the bottom of the plates in 10 ml of differentiation medium and further incubated for another 2 days. The nascent EBs were plated separately onto gelatin-coated 12-well plates and tested for pluripotency.

Immunofluorescence

For immunofluorescence, mouse iPSCs and EBs were fixed in 4% paraformaldehyde (PFA) for 10 minutes at room temperature, washed with phosphate-buffered saline (PBS), and permeabilized in 0.3% Triton X-100 in PBS for 10 minutes at room temperature. Primary antibodies used were anti-OCT4 (ab18976, Abcam, Cambridge, U.K.), anti-NANOG (NB100-58842, Novus Biologicals, Littleton, Colorado), anti-SOX2 (ab97959, Abcam), anti-SSEA1 (MC480, Cell signaling Technology, Beverly, MA), anti-NESTIN (ab11306, Abcam), anti-SMA (ab5694, Abcam), anti-AFP (MAB1368, R&D System, Minneapolis, MN) and anti-GATA-4 (ab134057, Abcam). After primary antibody incubation, samples were washed with PBS and incubated with secondary Alexa Fluor594-coniugated antibodies (Thermo Fisher Scientific), diluted 1:2,000. Samples were also counterstained with DAPI, 200 μg/ml. Slides were observed using an Olympus BX61 Research Microscope equipped with a cooled CCD camera. Images were captured and analyzed with Applied Imaging Software CytoVision.

DNA Sample Preparation and Genomic PCR Analysis

Genomic DNA was extracted from cell lines using QIAamp® DNA Kit (Qiagen, Germantown, MD) according to manufacturer's recommendations. For primer pairs and PCR conditions to amplify *wt* and *Cybb*$^-$ alleles see Jackson lab (https://www2.jax.org/protocolsdb/f?p=116:5:0::NO:5:P5_MASTER_PROTOCOL_ID,P5_JRS_CODE:22432,002365); primers for the analysis of informative single-nucleotide polymorphisms (SNPs) on the X chromosome are listed in Supporting Information Table S1. PCRs were performed under the following conditions: initial denaturing for 5 minutes at 94°C; denaturing for 30 seconds at 94°C, 55°C for 30 seconds, extension for 30 seconds at 72°C, repeated 35 times; final extension 5 minutes at 72°C. The PCR products were recovered using NucleoSpin® Gel and PCR Clean-up (Macherey-Nagel) and sequenced with specific primers.

Teratoma Formation and Histology

To produce teratomas, 5 × 10^6 mouse iPSCs were inoculated subcutaneously into the flank of 6-week-old NSG. After approximately 3 weeks, resected teratomas were fixed in formalin, processed for paraffin embedding and then stained with hematoxylin and eosin (H&E), following standard procedures.

Phagocyte Differentiation Protocol

For phagocyte differentiation protocol, EBs were generated through the "hanging drops" method in iPSC medium without LIF [21]. Two days after, EBs were pooled in low attachment conditions and after 4 days they were seeded on gelatine-coated 96-well plates. After 24 hours mouse hematopoietic cytokines were added (IL-3 and IL-6, 5 ng/ml, both from Peprotech, and G-CSF 10 ng/ml from Miltenyi Biotech, San Diego, CA) and after 3 days, the hematopoietic differentiation medium was replaced with doubled concentration of all cytokines. Half of the medium was replaced every 2 days. cKit$^+$ precursors were immuno-magnetically purified (MS columns with anti-mouse-CD117 MicroBeads, Miltenyi Biotec) at 14–18

days and seeded in complete methylcellulose-based medium (MethoCult GF M3534, Stem Cell Technologies, Vancouver, Canada) with the addition of 20 ng/ml of G-CSF for colony-forming unit (CFU) assays. Myeloid colonies were observed after approximately 10–14 days of culture, and at day 28–32, cells were collected and cytospun (800 rpm for 6 minutes; Shandon Cytospin 4, Thermo Fisher Scientific). The different cell types were evaluated after May–Grunwald Giemsa (MGG) staining (Carlo Erba, Milano, Italy).

Flow Cytometry

Dead cell discrimination was performed with LIVE/DEAD Fixable Dead Cell Stain Kit (ThermoFisher Scientific), following manufacturer instructions. Staining of cells for flow cytometry analysis was performed in PBS containing 2% FCS and 1 mM EDTA, with the following anti-mouse conjugated monoclonal antibodies: cKit (2B8), CD11b (M1/70), CD115 (AFS98), Ly6G (1A8-Ly6G; all from eBioscience, San Diego, CA) and CD45 (30/F11, from Biolegend). LSR Fortessa flow cytometer (BD Biosciences, San Jose, CA) equipped with BD FACSDIVA software (BD, Franklin Lakes, NJ) was used for data acquisition and FlowJo software (Tree Star, Inc., Ashland, OR) was used for data analysis.

Immunohistochemistry

Immunohistochemical assays were performed on cytospin preparations of differentiated mouse iPSCs. Cells were fixed in 4% PFA for 10 minutes at room temperature, washed with PBS, and then treated with 0.3% H_2O_2 for 15 minutes. After PBS washing, cells were fixed with Rodent Block M (RBM961L, Biocare Medical, Pacheco, CA) for 30 minutes at room temperature. Primary antibody used was anti-GP91 (1:100, BD Biosciences). After washing, cells were treated with MM HRP Polymer (Biocare Medical) for 30 minutes and then with Betazoid DAB (Biocare Medical) for 5 minutes. After washing, cells were counterstained with hematoxylin for 2 minutes, dehydrated and mounted.

NitroBlue Tetrazolium Assay

NitroBlue tetrazolium (NBT) assay was performed as previously described with minor modifications [22]. Briefly, methylcellulose wells containing CFUs were overlaid with one-fifth volume of NBT-saturated RPMI-1640 medium (Sigma–Aldrich) containing 500 ng/ml Phorbol 12-myristate 13-acetate (PMA, Sigma–Aldrich) and 5% bovine serum albumin (H2B) and incubated at 37°C for 30 minutes. CFUs were subsequently analyzed using inverted microscope (CKX31, Olympus), and the CFUs displaying blue formazan precipitates were scored as positive. CFU cells were recovered, pooled, and cytospun (800 rpm for 6 minutes; Thermo Fisher Scientific) and the formazan deposits were identified. Nuclei were counterstained with DAPI and acquired in fluorescence whereas dark formazane precipitates were analyzed in brightfield using an Olympus BX61 Research Microscope equipped with a cooled CCD camera. The two images were then merged.

Neutrophil Extracellular Trap Induction

To detect neutrophil extracellular trap (NET) formation, cells from CFU assays were recovered, pooled, and resuspended in Hanks' balanced saline solution (HBSS; Lonza). 1×10^5 cells were seeded on poly-L-lysine-coated glass coverslips in 12-well tissue-culture plates and allowed to settle for at least 30 minutes prior to stimulation. Cells were left unstimulated or treated with 500 ng/ml PMA (Sigma–Aldrich) in HBSS and incubated at 37°C for 120/180 minutes. Cells were fixed with an equal volume of 4% PFA added to the HBSS medium for 15 minutes. After washing with PBS, the samples were counterstained with DAPI, 200 μg/ml. Slides were observed using an Olympus BX61 Research Microscope equipped with a cooled CCD camera. Images were captured and analyzed with Applied Imaging Software CytoVision.

Statistical Analysis

Statistical analysis was performed using one-way analysis of variance with Tukey's post-test for grouped analysis and multiple comparisons with GraphPad Prism 6.0 (GraphPad Softwares, Inc., La Jolla, CA). Statistical significance was considered when $p < .05$ (*, $p < .05$; **, $p < .01$; ***, $p < .001$). All the experiments were performed in triplicate. All data are presented as mean ± SD.

Results

Experimental Design

To correct CGD derived cells, we designed a three step strategy (Fig. 1): (1) selectable CGD-iPSCs were generated from a mouse model (*Cybb*$^-$); (2) CT was performed on these cells via MMCT and diploid cells, in which the defective X chromosome has been substituted with a normal donor one, were selected; (3) cells were differentiated toward functional granulocytes.

Generation of iPSCs from the CGD Mouse Model

The *Cybb*$^-$ mutant mouse bears the *Cybb* gene inactivated by homologous recombination and recapitulates the human CGD phenotype [11]. The *CYBB* gene (also called *GP91*) is localized on the X chromosome and it is the most frequently mutated gene in the CGD human pathology. After crossing *Cybb*$^-$ mice with GFP$^+$ C57BL/6 mice, we isolated cKit$^+$ hematopoietic progenitors cells from the BM of a *Cybb*$^-$/GFP$^+$ male mouse. We generated iPSC lines by infecting progenitors cells with the four Yamanaka reprogramming factors hOCT4, hSOX2, hKLF4, and hc-MYC [17] using the integration-free Sendai virus gene-delivery method [23]. Several CGD-iPSC clones were isolated and characterized. The clone CGD-33, showed a normal diploid karyotype (Supporting Information Fig. S1A) and the presence of the *Cybb* mutation was confirmed by PCR analysis (Supporting Information Fig. S1B). The clone was bona fide pluripotent as assessed by colony morphology, by alkaline phosphatase assay and by the presence of stemness markers (Supporting Information Fig. S1C–S1E). Its ability to differentiate toward the three germ layers in vitro and to develop teratomas in vivo upon subcutaneous injection into NSG mice was also demonstrated (Supporting Information Fig. S1F, S1G). We also generated iPSC lines from a male GFP$^+$ C57BL/6 *wt* mouse as control (not shown).

Hprt Inactivation by CRISPR/Cas9 in CGD iPSCs

To obtain the correction of CGD genetic defect in the established mouse CGD-iPSC lines, we applied the CT protocol (Fig. 1) recently set up in mouse ESCs [1]. As recipient cell line, we used the CGD-33 clone in which we inactivated the endogenous *Hprt* gene through CRISPR technology [24], by targeting exon 3 with a

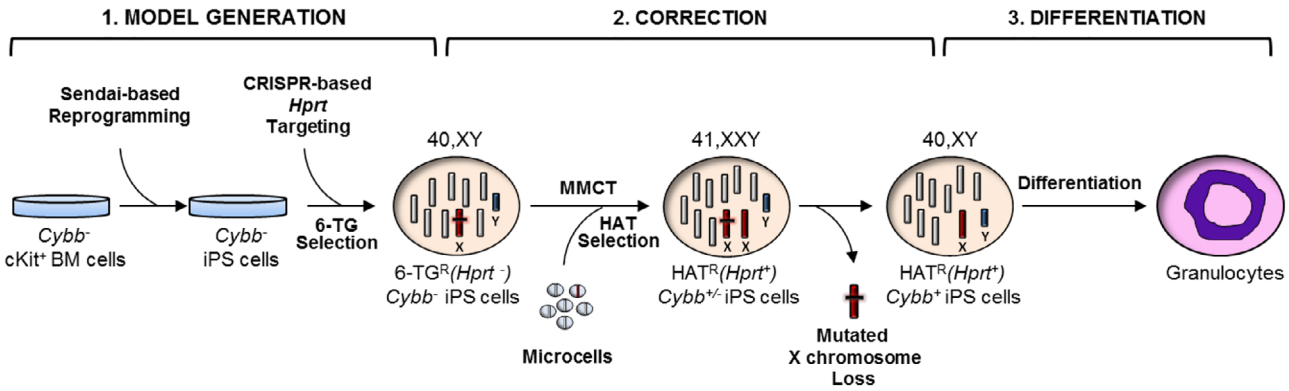

Figure 1. Schematic overview of the "chromosome therapy" approach in CGD-iPSCs. The scheme shows the step-by-step procedure followed to generate and correct mouse CGD-iPSCs in which an endogenous chromosome is replaced with an exogenous normal one. (1): Model generation: cKit$^+$ bone marrow cells were obtained from a male CGD mouse and reprogrammed to iPSCs. Their *Hprt* gene was targeted by CRISPR/Cas9 and *Hprt*$^-$ cells were selected in 6-TG medium. (2): Correction: the 6-TG^R cells were subjected to MMCT and X-transplanted clones were selected in HAT medium; subsequently, XY diploid iPSCs in which the endogenous X chromosome has been substituted with an exogenous normal one were obtained. (3): Differentiation: diploid XY corrected cells were differentiated toward mature granulocytes. Abbreviations: 6-TG selection, selection in 6-thioguanine medium; BM, bone marrow; CGD, chronic granulomatous disease; *Cybb*$^-$ mouse, mouse model of X-linked CGD; iPSC, induced pluripotent stem cell; HAT selection, selection in hypoxanthine–aminopterin–thymidine medium; *Hprt*, hypoxanthine phosphoribosyltransferase; MMCT, microcell mediated chromosome transfer.

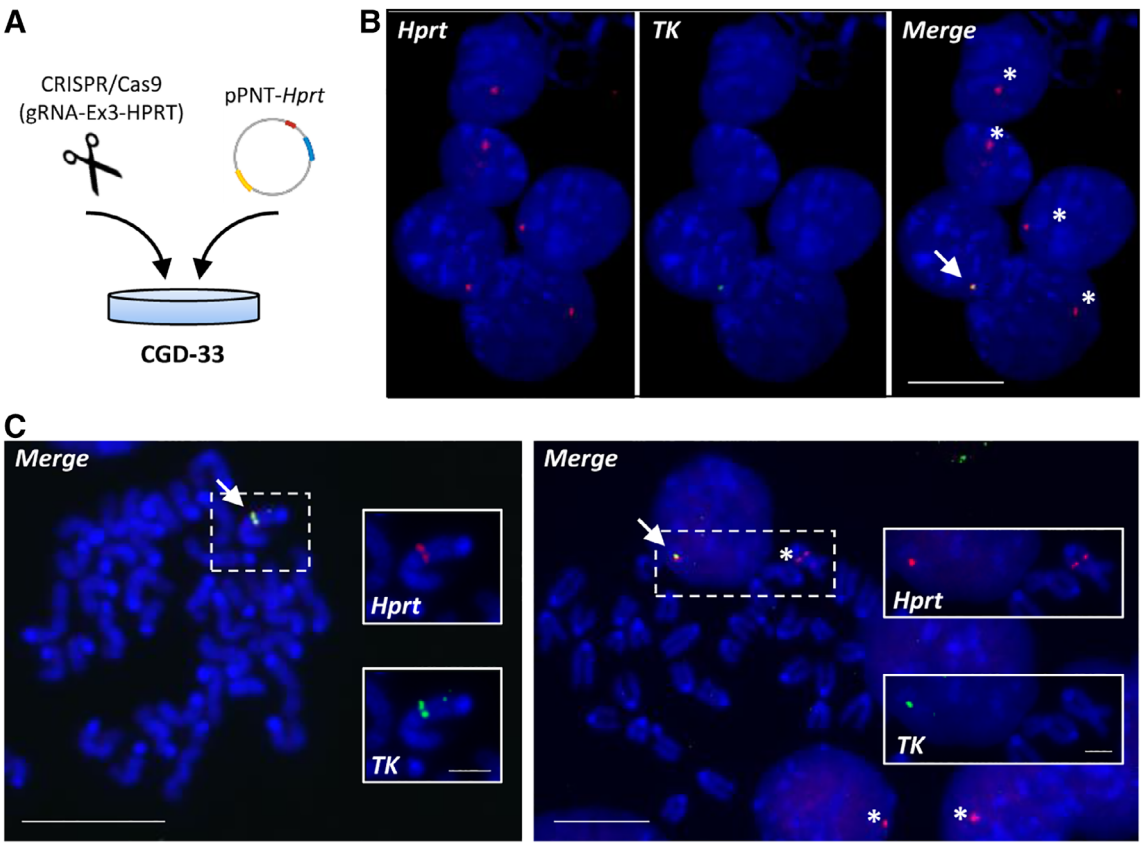

Figure 2. *Hprt* inactivation of the CGD-33 clone. **(A):** Schematic representation of the cotransfection strategy: CGD-induced pluripotent stem cells were cotransfected with a CRISPR/Cas9 plasmid containing a RNA guide specific for the exon 3 of the *Hprt* gene (gRNA-Ex3-*Hprt*) together with the pPNT-HPRT construct containing the HSV-TK gene (see Materials and Methods for details). **(B, C):** Representative images of interphase nuclei (B) and metaphase spreads (C) from transfected 6-TG^R CGD-33 cell pool after FISH. The BAC RP23-173F3 (red) containing the *Hprt* gene and the pPNT vector (green) containing only the HSV-TK gene (without the *Hprt* flanking regions) were used as probes. Scale bar: 10 μm. In (C) panel, insets are derived from regions identified by the dashed box. Scale bar: 2 μm. The asterisks (*) indicate sites where only the red signal is present. The arrow indicates the colocalized signals. Chromosomes were counterstained by DAPI (blue). Abbreviations: 6-TG, selection in 6-thioguanine medium; CGD, chronic granulomatous disease.

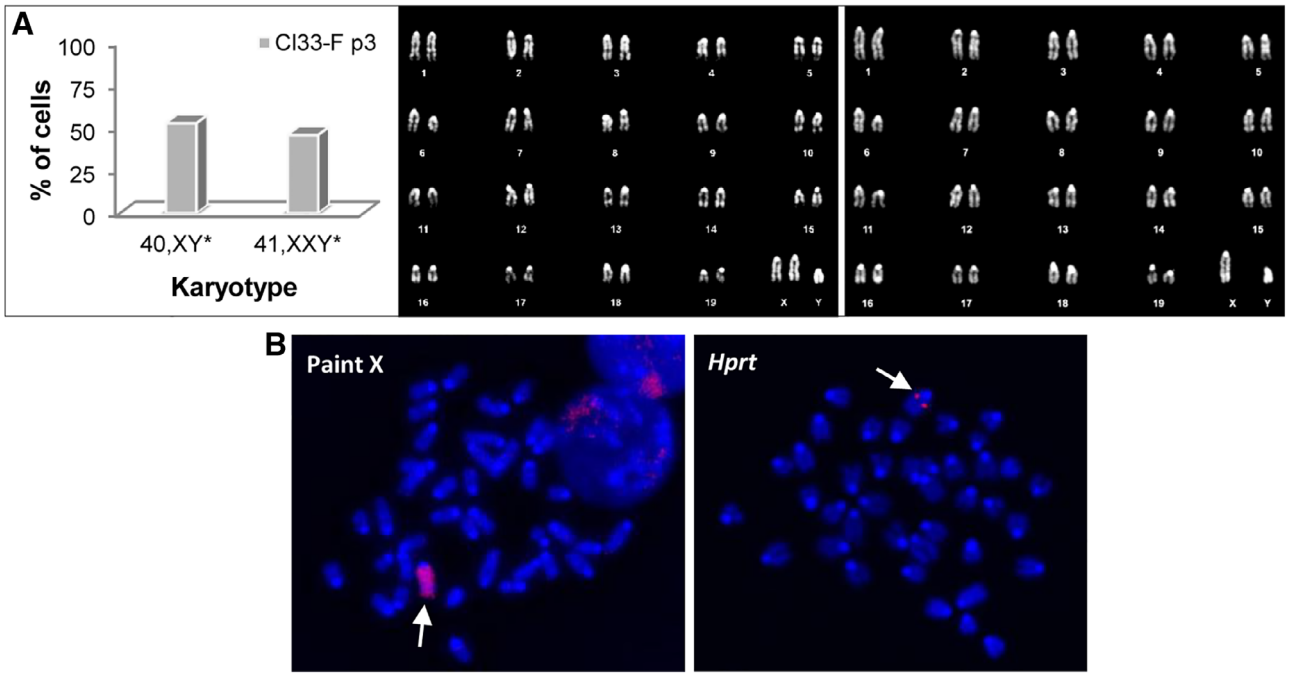

Figure 3. Analysis of the chromosome-transplanted HAT^R cl33-F clone. **(A):** Histogram showing the chromosome distribution (left) and representative DAPI-banding karyotypes at passage 3 (p3) of the two 41,XXY (middle) and 40,XY (right) cell populations. The asterisk (*) in the histogram indicates the presence of a deletion of the distal region of the chromosome 6. **(B):** Representative metaphase spreads after FISH on metaphase cells from the HAT^R cl33-F at passage 6 using the X-chromosome painting (red) and the BAC RP23-173F3 containing the *Hprt* gene (red) as probes. Arrows indicate the sites of hybridization signals. Chromosomes were counterstained with DAPI (blue).

specific gRNA (gRNA-Ex3-*Hprt*), to take advantage of the HAT/6-TG positive/negative selection system. Concomitantly, the pPNT-HPRT plasmid the HSV-TK gene, was cotransfected in order to exploit the TK/ganciclovir system for the elimination of the endogenous X chromosome, as previously described in Down syndrome iPSCs [5] (Fig. 2A; see Materials and Methods for details). The resultant 6-TG resistant (6-TG^R) cells, in which the *Hprt* allele was disrupted, were isolated and analyzed by FISH, to confirm the correct pPNT-HPRT plasmid insertion [18]. Twenty-two percentage of cells was found to display a correct colocalization (Fig. 2B, 2C).

CT in *Hprt*$^-$ Defective CGD iPSCs

The pool of *Hprt*$^-$ (6-TG^R) CGD-33 iPSCs was used as recipient cells and subjected to fusion experiments together with microcells from the A9/MEF-C12 cell line, containing a normal X chromosome [1]. Upon HAT selection, which eliminates *Hprt*$^-$ cells, five independent HAT resistant (HAT^R) clones (cl33-A, cl33-B, cl33-C, cl33-F, and cl33-G) with an efficiency of approximately one corrected clone per 2 million cells were obtained. As expected, in all HAT^R clones, two X chromosomes were detected, one endogenous and one microcell-derived containing the normal *Hprt* gene, except for the cl33-G clone in which only one X chromosome was present. This last clone, that likely had spontaneously lost the endogenous mutated X chromosome, displayed a tendency to lose also the Y chromosome and was excluded from further studies (data not shown). Clones 33A, 33B, and 33C were XXY but showed an aberrant karyotype and were excluded from further studies. Interestingly, in the cl33-F clone, a subpopulation with a normal content of 40 chromosomes was also present at passage 3 (Fig. 3A), indicating that loss of the mutated endogenous X chromosome had spontaneously occurred. After few passages in HAT selective medium, the presence of the normal exogenous X chromosome was further confirmed by FISH experiments using both a whole X chromosome painting and a BAC containing the *Hprt* gene as probes (Fig. 3B). By limiting dilution, several subclones with a XY diploid chromosome content were isolated making the ganciclovir selection unnecessary, as reported to occur in one of the two studies working on iPSC trisomic for chromosome 21 [6]. Karyotype analysis of all subclones revealed an overall normal chromosome distribution, with the exception of a deletion of the distal region of the chromosome 6, which is one of the chromosome mutations that spontaneously occur in pluripotent cells during long-term cultures [25–27]. Retrospective analysis confirmed that this cytogenetic aberration was not due to the CT procedure since it was absent in the original CGD-33 iPSC line but was already present in the 6-TG resistant pool of cells, in which the *Hprt* gene was inactivated by CRISPR/Cas9 before MMCT. Since the aim of this study was to establish a proof of principle for our approach, we decided to use these cells to demonstrate the correction of the *Cybb* genetic defect, despite the chromosome rearrangement.

Chromosome-Transplanted iPSC Clones Can Be Differentiated into Functional Granulocytes

In three corrected transplanted subclones (cl33-F8, cl33-F3, and cl33-F7) we first analyzed their karyotype and the *Cybb* gene by PCR analysis, confirming that XY diploid cells maintained only the *wt* allele (Fig. 4A, 4B and Supporting Information Fig. S2A,

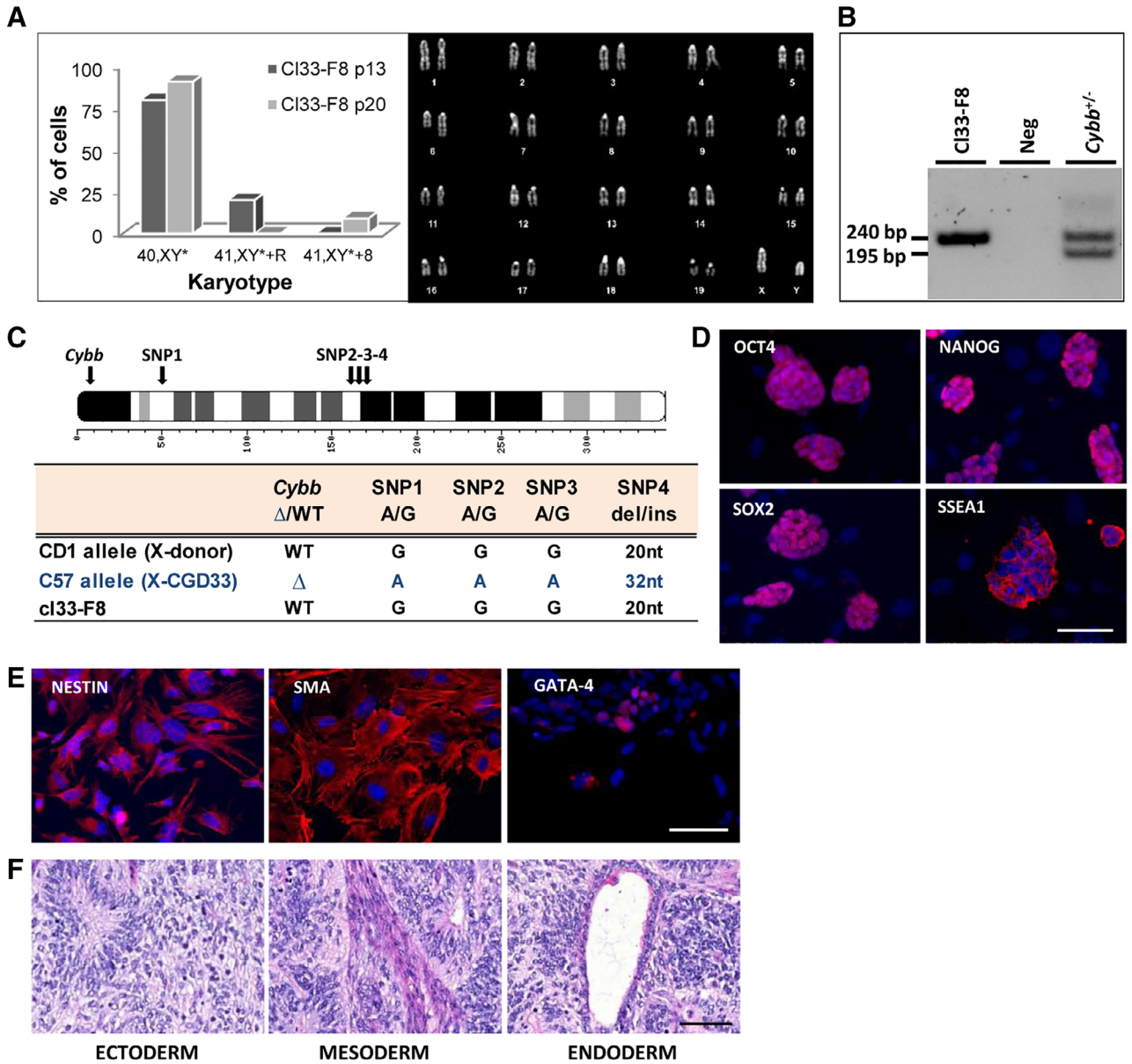

Figure 4. Characterization of the corrected cl33-F8 clone. **(A):** Left: histogram showing the chromosome distribution at passages 13 (p13) and 20 (p20). Right: representative DAPI-banding karyotype. The asterisk (*) in the histogram indicates the presence of a deletion of the distal region of the chromosome 6. **(B):** Analysis of the *Cybb* locus in the cl33-F8 and an heterozygous female *Cybb*$^{+/-}$ mouse DNA. Only the normal 240 bp band is seen in the transplanted cl33-F8. **(C):** Informative single-nucleotide polymorphism (SNP) analysis in the corrected cl33-F8 and uncorrected chronic granulomatous disease (CGD)-33 clone. Top: localization of the SNPs on the X chromosome. Bottom: SNP genotype in the endogenous (CGD strain, C57) and exogenous (donor strain, CD1) X chromosome showing that cl33-F8 bears only CD1 derived SNPs. **(D):** Immunostaining for stemness markers (red): OCT4, NANOG, SOX2, and SSEA1. Nuclei are counterstained with DAPI (blue). Scale bar: 50 μm. **(E):** Immunostaining for markers of the three germ layers (red): ectoderm (NESTIN), mesoderm (SMA), and endoderm (GATA-4). Nuclei are counterstained with DAPI (blue). Scale bar: 50 μm. **(F):** Teratoma formation assay. H&E stainings show primitive and mature neuroepithelium (ectoderm), mesenchymal cells (mesoderm), and gland-like structure (endoderm). Scale bar: 50 μm. Abbreviations: +R, not defined rearranged chromosome; +8, trisomy 8; Neg, negative control.

S2B). To confirm the CD1-derivation of the X chromosome, informative SNPs spanning the X chromosome were analyzed [1] (see Materials and Methods for details). As expected, all SNPs revealed CD1-derived allelic forms (Fig. 4C and Supporting Information Fig. S2C). Importantly, after the CT procedure, the three subclones have maintained their stemness: all clones were still pluripotent as assessed by their ability to differentiate in vivo toward the three germ layers, and to form teratomas upon subcutaneous injection into NSG mice (Fig. 4D, 4F and Supporting Information Fig. S2D–S2F).

The three corrected clones were differentiated to demonstrate that their cells have acquired the ability to differentiate into functional mature granulocytes. For this purpose, we set up a three-step differentiation protocol using a *wt* mouse iPSC clone (Supporting Information Fig. S3). Step 1, iPSCs were induced to an initial spontaneous differentiation through

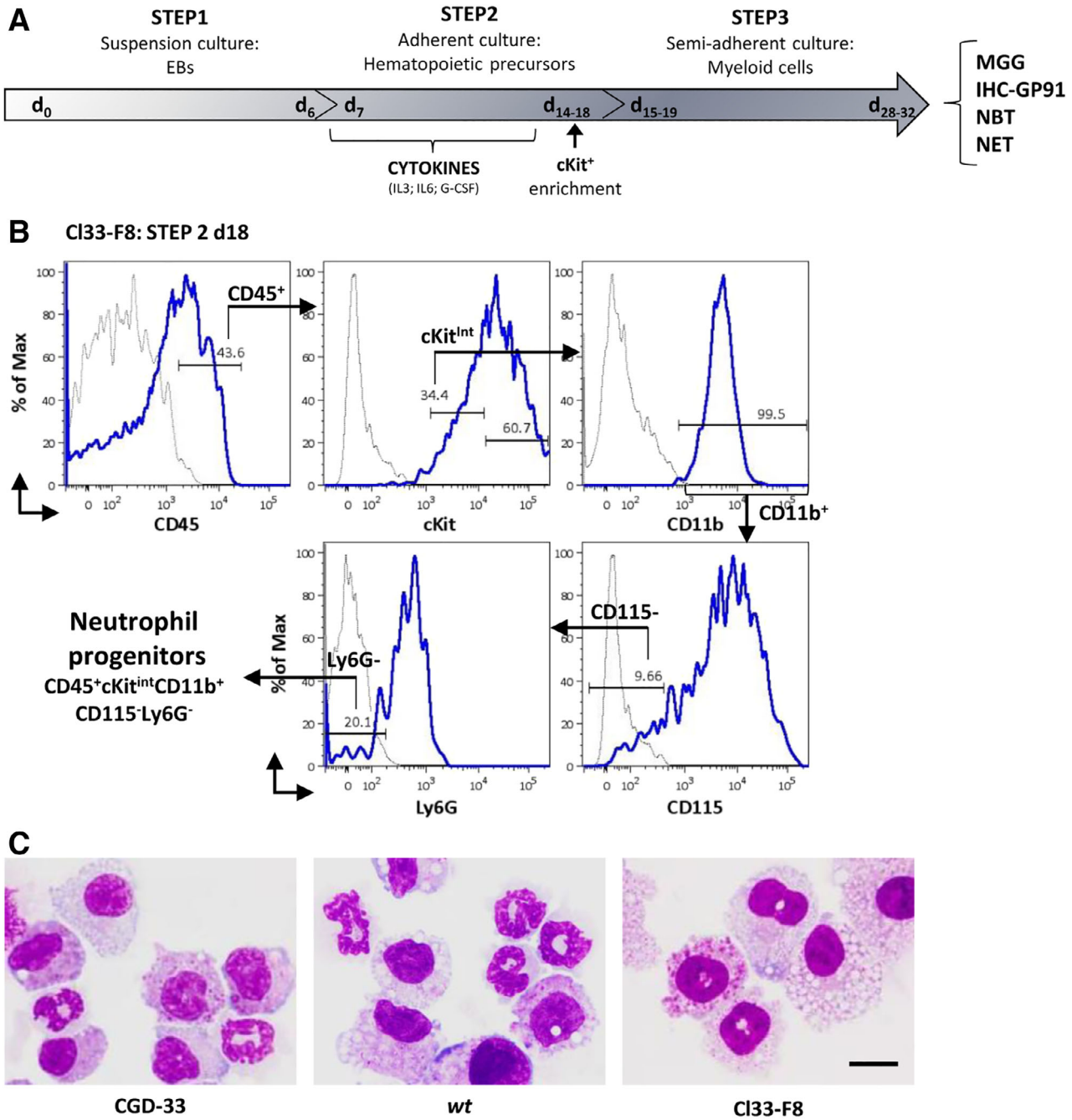

Figure 5. Granulocyte differentiation from induced pluripotent stem cells (iPSCs). **(A):** Schematic three-step differentiation protocol of mouse corrected CGD-iPSCs into granulocytes. Step 1: EB formation from day 0 to day 6 in suspension plates. Step 2: EB culture on adherent gelatin-coated plates in hematopoietic differentiation medium from day 7 to 14–18 days. Cytokines were added at day 7 and after 3 days their concentration was doubled. Step 3: Mature differentiation of cKit$^+$ purified hematopoietic in semi-solid medium (MethoCult) for additional 14 days (d28-32). Myeloid colonies were recovered and cytospin preparation were used to perform MGG, IHC-GP91, NBT, and NET assays. **(B):** Representative flow cytometry analysis for characterization of early neutrophil progenitors during the adherent culture conditions (step 2, day 18). The gray histogram represents the isotype control while the blue histogram is the fluorescent antibody staining for CD45, cKit, CD11b, CD115, and Ly6G. **(C):** Representative examples of MGG staining of CGD-33 clone (left), *wt* clone (middle), and the corrected cl33-F8 clone (right). Scale bar: 10 μm. Abbreviations: CGD, chronic granulomatous disease; EB, embryoid body; IHC, immunohistochemistry for GP91 protein; MMG, May–Grunwald Giemsa; NBT, NitroBlue tetrazolium assay; NET, neutrophil extracellular trap; *wt*, wild-type.

embryoid body (EB) generation by the "hanging drop" method [21]; step 2, after 6 days of suspension culture, EBs were seeded on gelatin-coated tissue-culture wells in hematopoietic differentiation medium supplemented with mouse hematopoietic cytokines (IL-3, IL-6, and G-CSF) for additional 12 days. By a time-course flow cytometry analysis, we identified the day within step 2 when the highest yield of granulocyte precursors were achieved. To do this, we focused on the recently

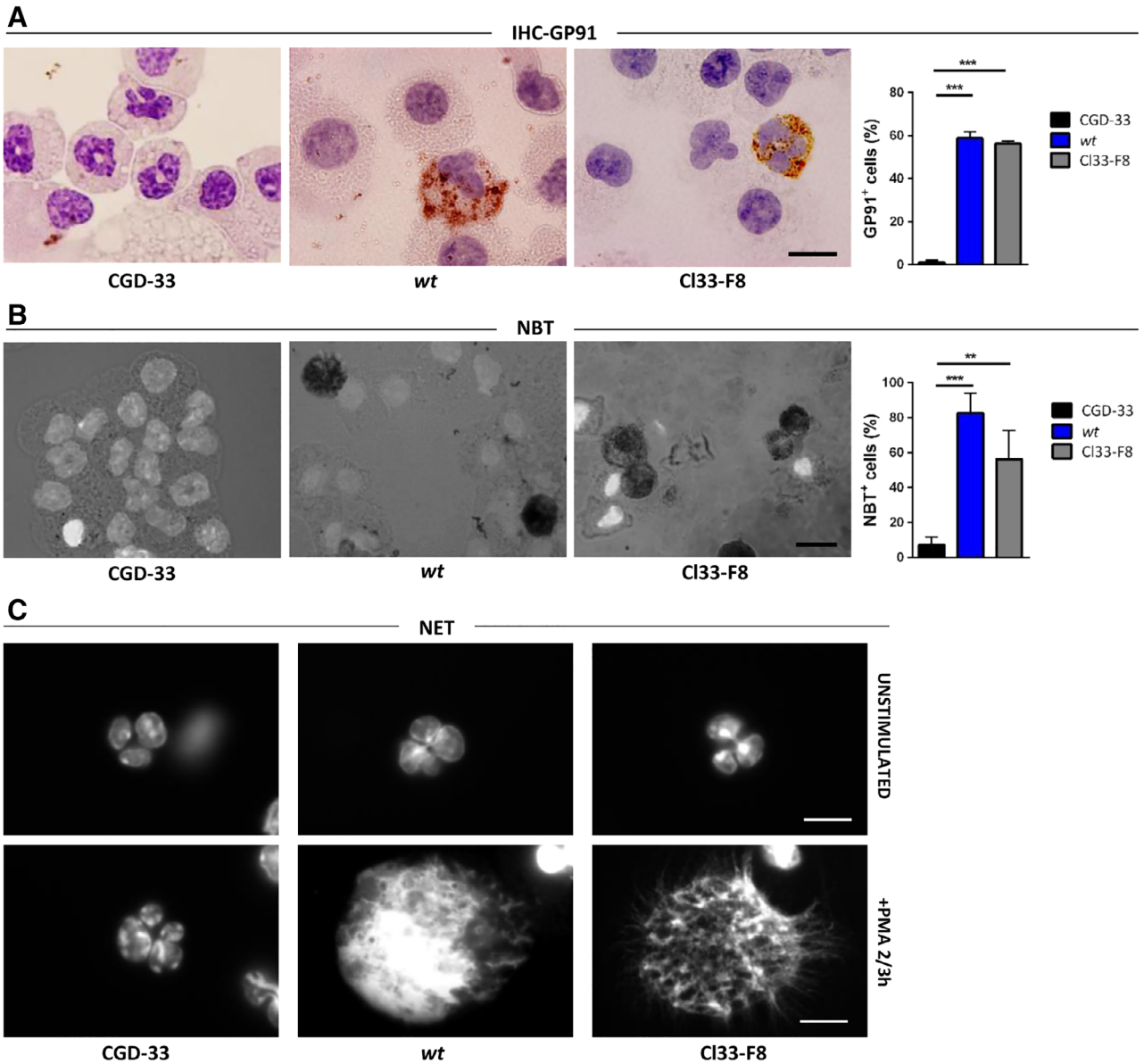

Figure 6. Analysis of differentiated cells from the defective CGD-33 clone (left), *wt* clone (middle), and the corrected cl33-F8 clone (right). **(A):** IHC with an antibody to GP91. The cells were counterstained with hematoxylin. Scale bar: 10 µm. The histogram shows the percentage of GP91 positive cells on the incorrect, *wt*, and corrected clones, respectively. ***, $p < .001$; $n = 3$. **(B):** NBT assay. The images are a merge of brightfield (dark-formazane precipitates) and fluorescence acquisitions (light gray-nuclei counterstained with DAPI). Scale bar: 10 µm. The histogram shows the percentage of the NBT positive cells performed on the incorrect, *wt*, and corrected clones, respectively. **, $p < .01$; ***, $p < .001$; $n = 3$. **(C):** NET assay. Representative image of differentiated cells in absence (upper) or presence of PMA (lower). Nuclei are counterstained with DAPI. Scale bar: 10 µm. Abbreviations: CGD, chronic granulomatous disease; IHC, immunohistochemistry; NBT, NitroBlue tetrazolium assay; NET, neutrophil extracellular trap; *wt*, wild-type.

characterized early proliferative neutrophil progenitors that are able to generate colony-forming unit granulocyte (CFU-G) in methylcellulose-based medium [28–30]. Flow cytometry analysis using anti-CD45, cKit, CD11b, CD115, Ly6G antibodies revealed that the highest frequency of $CD45^{+}cKit^{int}CD11b^{+}CD115^{-}Ly6G^{-}$ neutrophil progenitors, was obtained at 14–18 days (Supporting Information Fig. S3B, S3C). In step 3, purified $cKit^{+}$ cells containing the highest number of neutrophil progenitors were plated in methylcellulose-based medium (MethoCult), with the addition of mouse G-CSF, to promote the differentiation toward granulocytes and to evaluate the myeloid colony formation. Myeloid colonies were observed after approximately 10–14 days of culture. Finally, colonies were picked up and pooled, and the morphology and functionality of the differentiated cells were analyzed.

The differentiation protocol was then applied to the uncorrected and corrected CGD clones (Fig. 5A). As expected, in the corrected cl33-F8, the presence of neutrophil progenitors at day 18 was confirmed by flow cytometry analysis (Fig. 5B). MGG staining of cytospin preparations of the differentiated myeloid colonies revealed the presence of granulocytes at different stages of maturation in *wt*, uncorrected, CGD-33, and the three corrected cl33-F3, cl33-F7, cl33-F8 iPSC clones (Fig. 5C and Supporting Information Fig. S4A, S4B).

We tested the rescue of GP91 protein by immunohistochemistry: whereas in mature granulocytes differentiated from the *wt* and the corrected cl33-F8 clone the protein was specifically detected, only minimal reactivity was found in the uncorrected CGD-33 clone (Fig. 6A). In detail, Diaminobenzidine (DAB) precipitates ($GP91^+$) were found in more than 50% of differentiated mature granulocytes from the *wt* and corrected cells, whereas those derived from the uncorrected clone showed positivity in less than 2%. Importantly, to test the functionality of the differentiated cells, the NBT assay, allowing the detection of the reactive oxygen species (ROS), was performed on cl33-F8, cl33-F3, and cl33-F7. In all corrected clones as well as in the *wt* iPSCs, formazan precipitates were observed, whereas, as expected, they were not present in the differentiated uncorrected CGD-33 clone (Fig. 6B and Supporting Information Fig. S4A, S4B).

Furthermore, the NET assay was also performed. Neutrophils kill pathogens by phagocytosis, degranulation, and/or the release of web-like structures called NETs that trap and kill microbes. Neutrophils from CGD patients, who carry mutations inactivating the NADPH oxidase, do not form NETs [31]. In PMA-stimulated granulocytes differentiated from the corrected cl33-F8, as well as from the *wt*, NET formation was observed, whereas, as expected, it did not occur in the differentiated uncorrected CGD-33 (Fig. 6C). NET formation in the PMA stimulated granulocytes differentiated from the other two corrected clones was also observed (Supporting Information Fig. S4A, S4B).

Together, these data demonstrate that we were able to obtain functional granulocytes and that the CT protocol is a good approach to correct this kind of genetic defect involving the X chromosome.

Discussion

The recent introduction, among gene therapy options, of the programmed nucleases allows for a precise and efficient correction of the most frequent genetic defects [32–34]. However, even with the prodigious CRISPR technology, several chromosomal aberrations cannot be rescued. Among these, we can mention large deletions, aneuploidies, and other structural complex abnormalities which can be treated only by novel tools that can be defined as "chromosome" or "genomic therapy" [1, 35].

We have recently introduced the concept of CT, referring to the precise substitution of a defective endogenous chromosome with a normal exogenous one [1]. CT differs from chromosome transfer because, although initiated by the well-known technique of MMCT, it allows the generation of diploid normal cells which have potential for *quasi*-autologous cell-based therapies. Our previous experiments were performed on a mouse ESC in which an X chromosome bearing the *Hprt* mutation, responsible in humans for the Lesch–Nyhan disease, was successfully corrected by CT.

Here, we perform a second step toward the translation ability of this strategy, by performing a proof of principle study on a mouse model of X-linked CGD, a human immunodeficiency which has been the target of many attempts to gene therapy [36, 37]. Viral vector-based trials for gene correction in humans have been reported, but the occurrence of undesired events [38, 39] and the concomitant introduction of programmable nucleases prompted the investigation of "gene editing" approaches to more precisely correct the nucleotide defect in iPSCs or directly in hematopoietic stem cells. We must emphasize that correction of the CGD defect by programmable nucleases in iPSCs from mouse model as well as human patients has already been accomplished [40–44]. Likewise, production of functional granulocytes from corrected or noncorrected human and mouse CGD-iPSCs has already been reported [22, 45]. Recently, Cas9-mediated repair has been successful in correcting a missense mutation in hematopoietic stem cells from a CGD patient [46], but even this approach would not be satisfactory for the approximately 10%–15% of CGD patients with large deletions, who could benefit from the approach described here.

We generated iPSCs from the $Cybb^-$ mouse strain, inactivated the endogenous *Hprt* gene to provide a selectable marker, performed MMCT, and isolated X-transplanted clones by HAT selection which spontaneously lost the endogenous *Hprt* deficient X chromosome, thus restoring a XY diploid genome. These cells were later forced to differentiate toward granulocytes which were shown to be functional. Although the efficiency of the CT approach is quite low, the few generated iPSC clones can be expanded indefinitively toward the desired lineage. As with all the strategies based on iPSCs, there is still a long way to make this approach useful for the clinics, but we believe that our results establish an important proof of principle for the usefulness of this kind of genomic therapy in selected cases.

Conclusion

We demonstrated that with a previous inactivation of the *Hprt* gene, the CT approach can be applied to iPSCs derived from a CGD mouse model leaving no mark of the procedure. The same approach could be, in theory, applied to every disease located on the X chromosome. Among these, two relatively frequent defects, the DD, and the Fragile X, could particularly benefit from this approach. Recently, to cure the DD a CRISPR-based strategy consisting on the skipping of mutated exons has been proposed, but the resulting protein is not normal and the disease is not completely cured [7, 8]. On the contrary, our approach would allow a perfect restoration of the normal dystrophin protein with all the regulatory regions intact, although so far it can only be applied to iPSCs in vitro which cannot be administered directly in vivo. However, iPSCs can be differentiated to muscle cells and these could be inoculated in vivo, an approach pursued by many laboratories [47]. Although CT on human iPSCs has not yet been reported, recent improvements in MMCT [48] could allow overcoming this difficulty and give rise to progenies of autologous corrected cells from patients affected by these devastating diseases for which conventional therapies are still unsatisfactory.

Acknowledgments

This reasearch was supported by PNR-CNR Aging Program 2012–2014 to P.V. A.C. and C.M. are recipients of a fellowship from Fondazione Nicola del Roscio. S.M. is recipient of a fellowship from Fondazione Damiano per l'Ematologia. We thank Colin Sweeney, Veronica Marrella, and Michela Lizier for useful

suggestions; Cristina Sobacchi for careful reading of the article; Stefano Mantero for technical help.

Author Contributions

A.C.: collection and assembly of data, data analysis and interpretation, manuscript writing, final approval of manuscript; L.S., C.R., E.S., F.F.: collection and assembly of data, data analysis and interpretation, final approval of manuscript; C.M., S.M., E.C., D.S.: collection and assembly of data, final approval of manuscript; B.C., A.V.: data analysis and interpretation, final approval of manuscript; P.V.: conception and design, data analysis and interpretation, manuscript writing, final approval of manuscript; M.P.: conception and design, data analysis and interpretation, manuscript writing, final approval of manuscript.

Disclosure of Potential Conflicts of Interest

The authors indicated no potential conflicts of interest.

Data Availability Statement

The data that support the findings of this study are available from the corresponding author upon reasonable request.

References

1 Paulis M, Castelli A, Susani L et al. Chromosome transplantation as a novel approach for correcting complex genomic disorders. Oncotarget 2015;6:35218–35230.

2 Lupski JR. Genomic disorders: Structural features of the genome can lead to DNA rearrangements and human disease traits. Trends Genet 1998;14:417–422.

3 Kim T, Plona K, Wynshaw-Boris A. A novel system for correcting large-scale chromosomal aberrations: Ring chromosome correction via reprogramming into induced pluripotent stem cell (iPSC). Chromosoma 2017;126:457–463.

4 Bershteyn M, Hayashi Y, Desachy G et al. Cell-autonomous correction of ring chromosomes in human induced pluripotent stem cells. Nature 2014;507:99–103.

5 Li LB, Chang KH, Wang PR et al. Trisomy correction in Down syndrome induced pluripotent stem cells. Cell Stem Cell 2012;11:615–619.

6 Maclean GA, Menne TF, Guo G et al. Altered hematopoiesis in trisomy 21 as revealed through in vitro differentiation of isogenic human pluripotent cells. Proc Natl Acad Sci USA 2012;109:17567–17572.

7 Tabebordbar M, Zhu K, Cheng JKW et al. In vivo gene editing in dystrophic mouse muscle and muscle stem cells. Science 2016;351:407–411.

8 Long C, Li H, Tiburcy M et al. Correction of diverse muscular dystrophy mutations in human engineered heart muscle by single-site genome editing. Sci Adv 2018;4:eaap9004.

9 Park CY, Halevy T, Lee DR et al. Reversion of FMR1 methylation and silencing by editing the triplet repeats in fragile X iPSC-derived neurons. Cell Rep 2015;13:234–241.

10 Yen PH. X chromosome rearrangements. In: Lupski JR, Stankiewicz P, eds. Genomic Disorders: The Genomic Basis of Disease. New Jersey: The Humana Press, Inc., 2006:247–262.

11 Pollock JD, Williams DA, Gifford MA et al. Mouse model of X-linked chronic granulomatous disease, an inherited defect in phagocyte superoxide production. Nat Genet 1995;9:202–209.

12 Pellicciotta M, Rigoni R, Falcone EL et al. The microbiome and immunodeficiencies: Lessons from rare diseases. J Autoimmun 2019;98:132–148.

13 Chiriaco M, Di Matteo G, Sinibaldi C et al. Identification of deletion carriers in X-linked chronic granulomatous disease by real-time PCR. Genetic Test Mol Biomarkers 2009;13:785–789.

14 Royer-Pokora B, Kunkel LM, Monaco AP et al. Cloning the gene for an inherited human disorder—Chronic granulomatous disease—On the basis of its chromosomal location. Nature 1986;322:32–38.

15 Dinauer MC, Orkin SH, Brown R et al. The glycoprotein encoded by the X-linked chronic granulomatous disease locus is a component of the neutrophil cytochrome b complex. Nature 1987;327:717–720.

16 Okabe M, Ikawa M, Kominami K et al. "Green mice" as a source of ubiquitous green cells. FEBS Lett 1997;407:313–319.

17 Takahashi K, Tanabe K, Ohnuki M et al. Induction of pluripotent stem cells from adult human fibroblasts by defined factors. Cell 2007;131:861–872.

18 Paulis M, Castelli A, Lizier M et al. A prescreening FISH-based method to detect CRISPR/Cas9 off-targets in mouse embryonic stem cells. Sci Rep 2015;5:12327.

19 Susani L, Alessandra C, Michela L et al. Correction of a recessive genetic defect by CRISPR-Cas9-mediated endogenous repair. The CRISPR J 2018;1:230–238.

20 Paulis M, Bensi M, Orioli D et al. Transfer of a human chromosomal vector from a hamster cell line to a mouse embryonic stem cell line. Stem Cells 2007;25:2543–2550.

21 Neri T, Muggeo S, Paulis M et al. Targeted gene correction in osteopetrotic-induced pluripotent stem cells for the generation of functional osteoclasts. Stem Cell Rep 2015;5:558–568.

22 Mukherjee S, Santilli G, Blundell MP et al. Generation of functional neutrophils from a mouse model of X-linked chronic granulomatous disorder using induced pluripotent stem cells. PLoS One 2011;6:e17565.

23 Fusaki N, Ban H, Nishiyama A et al. Efficient induction of transgene-free human pluripotent stem cells using a vector based on Sendai virus, an RNA virus that does not integrate into the host genome. Proc Jpn Acad B Phys Biol Sci 2009;85:348–362.

24 Urnov FD. Genome editing B.C. (before CRISPR): Lasting lessons from the "Old Testament". Crispr J 2018;1:34–46.

25 Rebuzzini P, Neri T, Mazzini G et al. Karyotype analysis of the euploid cell population of a mouse embryonic stem cell line revealed a high incidence of chromosome abnormalities that varied during culture. Cytogenet Genome Res 2008;121:18.

26 D'Hulst C, Parvanova I, Tomoiaga D et al. Fast quantitative real-time PCR-based screening for common chromosomal aneuploidies in mouse embryonic stem cells. Stem Cell Rep 2013;1:350–359.

27 Kim YM, Lee JY, Xia L et al. Trisomy 8: A common finding in mouse embryonic stem (ES) cell lines. Mol Cytogenet 2013;6:3.

28 Zhu YP, Padgett L, Dinh HQ et al. Identification of an early unipotent neutrophil progenitor with pro-tumoral activity in mouse and human bone marrow. Cell Rep 2018;24:2329.e2328–2341.e2328.

29 Kim MH, Yang D, Kim M et al. A late-lineage murine neutrophil precursor population exhibits dynamic changes during demand-adapted granulopoiesis. Sci Rep 2017;7:39804.

30 Evrard M, Kwok IWH, Chong SZ et al. Developmental analysis of bone marrow neutrophils reveals populations specialized in expansion, trafficking, and effector functions. Immunity 2018;48:364.e368–379.e368.

31 Fuchs TA, Abed U, Goosmann C et al. Novel cell death program leads to neutrophil extracellular traps. J Cell Biol 2007;176:231–241.

32 Mali P, Yang L, Esvelt KM et al. RNA-guided human genome engineering via Cas9. Science 2013;339:823–826.

33 Komor AC, Badran AH, Liu DR. CRISPR-based technologies for the manipulation of eukaryotic genomes. Cell 2017;168:20–36.

34 Doudna JA, Charpentier E. Genome editing. The new frontier of genome engineering with CRISPR-Cas9. Science 2014;346:1258096.

35 Plona K, Kim T, Halloran K et al. Chromosome therapy: Potential strategies for the correction of severe chromosome aberrations. Am J Med Genet C Semin Med Genet 2016;172:422–430.

36 Ott MG, Schmidt M, Schwarzwaelder K et al. Correction of X-linked chronic granulomatous disease by gene therapy, augmented by insertional activation of MDS1-EVI1, PRDM16 or SETBP1. Nat Med 2006;12:401–409.

37 Laugsch M, Rostovskaya M, Velychko S et al. Functional restoration of gp91phox-oxidase activity by BAC transgenesis and gene targeting in X-linked chronic granulomatous disease iPSCs. Mol Ther 2016;24:812–822.

38 Hacein-Bey-Abina S, Von Kalle C, Schmidt M et al. LMO2-associated clonal T cell proliferation in two patients after gene therapy for SCID-X1. Science 2003;302:415–419.

39 Stein S, Ott MG, Schultze-Strasser S et al. Genomic instability and myelodysplasia with monosomy 7 consequent to EVI1 activation after gene therapy for chronic granulomatous disease. Nat Med 2010;16:198–204.

40 Dreyer AK, Hoffmann D, Lachmann N et al. TALEN-mediated functional correction of X-linked chronic granulomatous disease in patient-derived induced pluripotent stem cells. Biomaterials 2015;69:191–200.

41 Flynn R, Grundmann A, Renz P et al. CRISPR-mediated genotypic and phenotypic correction of a chronic granulomatous disease mutation in human iPS cells. Exp Hematol 2015;43:838.e833–848.e833.

42 Merling RK, Sweeney CL, Chu J et al. An AAVS1-targeted minigene platform for correction of iPSCs from all five types of chronic granulomatous disease. Mol Ther 2015;23:147–157.

43 Zou J, Sweeney CL, Chou BK et al. Oxidase-deficient neutrophils from X-linked chronic granulomatous disease iPS cells: Functional correction by zinc finger nuclease-mediated safe harbor targeting. Blood 2011; 117:5561–5572.

44 Sweeney CL, Zou J, Choi U et al. Targeted repair of CYBB in X-CGD iPSCs requires retention of intronic sequences for expression and functional correction. Mol Ther 2017;25:321–330.

45 Jiang Y, Cowley SA, Siler U et al. Derivation and functional analysis of patient-specific induced pluripotent stem cells as an in vitro model of chronic granulomatous disease. Stem Cells 2012;30:599–611.

46 De Ravin SS, Li L, Wu X et al. CRISPR-Cas9 gene repair of hematopoietic stem cells from patients with X-linked chronic granulomatous disease. Sci Transl Med 2017;9:eaah3480.

47 Tedesco FS, Hoshiya H, D'Antona G et al. Stem cell-mediated transfer of a human artificial chromosome ameliorates muscular dystrophy. Sci Transl Med 2011;3:96ra78.

48 Suzuki T, Kazuki Y, Oshimura M et al. Highly efficient transfer of chromosomes to a broad range of target cells using Chinese hamster ovary cells expressing murine leukemia virus-derived envelope proteins. PLoS One 2016;11:e0157187.

See www.StemCells.com for supporting information available online.

